16th World Conference on Earthquake, 16WCEE 2017
Santiago Chile, January 9th to 13th 2017
Paper N° 1126 (Abstract ID)
Registration Code: S-Z1464643420

FROM A RISK-TARGETED REGIONAL EARTHQUAKE MODEL FOR SOUTH-EAST ASIA TO REGION SPECIFIC RISK MODELS

J. Woessner[(1)], E. Seyhan[(2)], M. Nyst[(3)]

[(1)] Lead Modeler, Risk Management Solutions Inc., Zurich, Switzerland, jochen.woessner@rms.com
[(2)] Senior Modeler, Risk Management Solutions Inc., Newark, CA, USA, emel.seyhan@rms.com
[(3)] Director, Risk Management Solutions Inc., Newark, CA, USA, marleen.nyst@rms.com

Abstract

The last decade has shown the social and economic vulnerability of countries in South-East Asia to earthquake hazard and risk. The 2004 M9.2 Sumatra earthquake and the associated tsunami caused significant casualties and economic losses generating major attention internationally due to the scale of its impact across the urban areas of South-East Asia and Indian Ocean (Indonesia, Thailand, Sri Lanka, and India). While many disaster mitigation programs to improve societal earthquake resilience are under way focusing on saving lives and livelihoods, the risk management sector is challenged to model economic consequences. We present the hazard component suitable for a South-East Asia earthquake risk model covering Indonesia, Malaysia, Singapore, Thailand, Vietnam and the Philippines. The consistent regional model builds upon refined modelling approaches for 1) background seismicity, i.e. earthquakes not occurring on mapped fault structures, 2) seismic activity from geologic and geodetic data on crustal faults and 3) along the interface of subduction zones. We elaborate on building rate model for crustal fault systems (e.g. Sumatra fault zone, Philippine fault zone) as well as the subduction zones and showcase its characteristics. We combine this with an up-to-date ground motion model that is suitable for this tectonically complex area. We assign more weights to globally developed ground motion prediction equations (GMPEs) due to the scarcity of strong ground motion data in Southeast Asia. We analyze the components of the risk model per country by computing the contributions by source type to typical risk metrics (return period losses, average annual loss) and considering the impact of the hazard model on all lines of business.

Keywords: Seismic risk; Seismic Hazard; South-East Asia; Average Annual Loss

1. Introduction

Over the past decades, the societies of many mainland and maritime countries in South-East have suffered several severe earthquake catastrophes in terms of human casualties, loss of livelihoods and economic losses. The 2004 M9.0 Andaman-Sumatra earthquake and the associated tsunami caused more than 225,000 fatalities, generating significant attention internationally due to the scale of its impact across the Indian Ocean. Overall economic losses from this one disaster were approximately US$10 billion, with the majority of loss attributed to tsunami damage in Indonesia, Thailand, Sri Lanka, and India.

The history of deadly earthquakes in South-East Asia rupturing either subduction zones or crustal faults is well documented. Earthquakes are often accompanied by cascading effects such as tsunamis, landslides, and liquefaction. Examples of recent destructive events on crustal faults along the Indonesian Islands include the December 1992 M7.8 Flores Earthquake with more than 2,500 fatalities, the May 2006 M7.7 Java-Yogyakarta Earthquake with more than 5,500 fatalities, and the September 2009 M7.9 Sumatra Earthquake with more than 1,000 fatalities. Similarly, the Philippines have experienced recent destructive earthquakes such as the August 1976 M8.0 Moro Gulf Earthquake on the trench southeast of Mindanao with more than 5,000 fatalities, and the July 1990 M7.8 Luzon Earthquake on the Philippines Fault with more than 1,600 fatalities, however, also faulting on previously unknown faults such as exemplified by the 2013 M7.2 Bohol earthquake threaten society. While less frequent, earthquakes are also an important hazard for Thailand, Malaysia and Vietnam, as shown by the 2014 M6.2 Mae Lao [27] and the 2015 M6.0 Sabah earthquake in Malaysia.

Seismic risk has increased due to rapidly growing populations and economies. The wider urban area of Jakarta, for example, today has the highest exposure density in Indonesia, is the most populated city in Southeast Asia

and the fastest growing among the world's emerging economies. Metropolitan Manila, another area of high exposure density, has the second largest economy in Southeast Asia and accounts for 33% of the Philippines' GDP, and a similar situation if found for Bangkok in Thailand. To worsen the situation, all of these Megacities are located largely in sedimentary basins with high shaking amplification and liquefaction potential; Manila spreads, for example, on soft lake sediments and across the Marikina Valley Fault system that is capable of hosting M7+ events (see Valley fault atlas of the Philippine Institute for Volcanology and Seismology, PhiVolcs). Due to the combination of inevitable natural hazards and the rapid growth of exposure throughout the region, it is imperative to assess the societal and economic impacts for the entire Southeast Asia region.

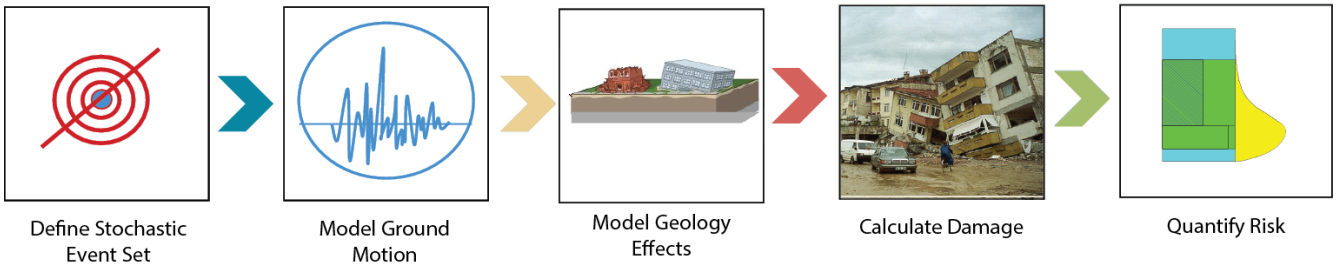

Fig. 1 - The four modules of seismic risk assessment (from left to right): The Stochastic Event Set module derived from the earthquake source model that characterizes long-term earthquake probabilities (rates); the Ground Motion Model with which the ground shaking spectral parameters are calculated for each event in the SES; liquefaction, soil amplification and landslide potential are then considered before the damage calculation module is applied to assess average damage and uncertainties; the financial model is then used to quantify the financial impact for all perspectives.

We approach this challenge with a modeling philosophy that values the nature of the all modules for risk assessment (Fig. 1). We focus on elaborating on the comprehensive earthquake hazard model. Rather than characterizing earthquake sources for single countries, we build the hazard component across the national boundaries and assess the earthquake rates disregarding human-imposed boundaries, thus build a comprehensive hazard model for the existing large tectonic system (Fig. 2 left). The same approach is taken to assess geotechnical parameters to assess soil amplification, liquefaction and landslide potential. While this is beneficial for the hazard assessment, it is important to include country-specific construction practices and cultural attitudes when assessing possible damage and quantifying risk metrics, both for mitigating risk for human lives and economic losses. This combined approach makes the model a unique for its application in the region and matches the approaches applied in other regions of the world.

1.1 Tectonic Setting

Southeast Asia spans a tectonically complex area, characterized by high seismic and volcanic activity. The region is exposed to seismic hazard and its triggered effects such as tsunamis and/or landslides, originating from the forces causing the convergence of the tectonic plates. The Sunda block is centered in the heart of Southeast Asia and defines a stable region covering large areas of Indonesia, Malaysia, Thailand, and the Indochina countries up to southern China. The Sunda block is surrounded by active subduction zones and interfaces with the Eurasian/ Indian plate to the west, the Australian plate to the South, the Philippine plate to the east, and the stable southern China block to the north (Simons et al, 2007; Bird, 2003).

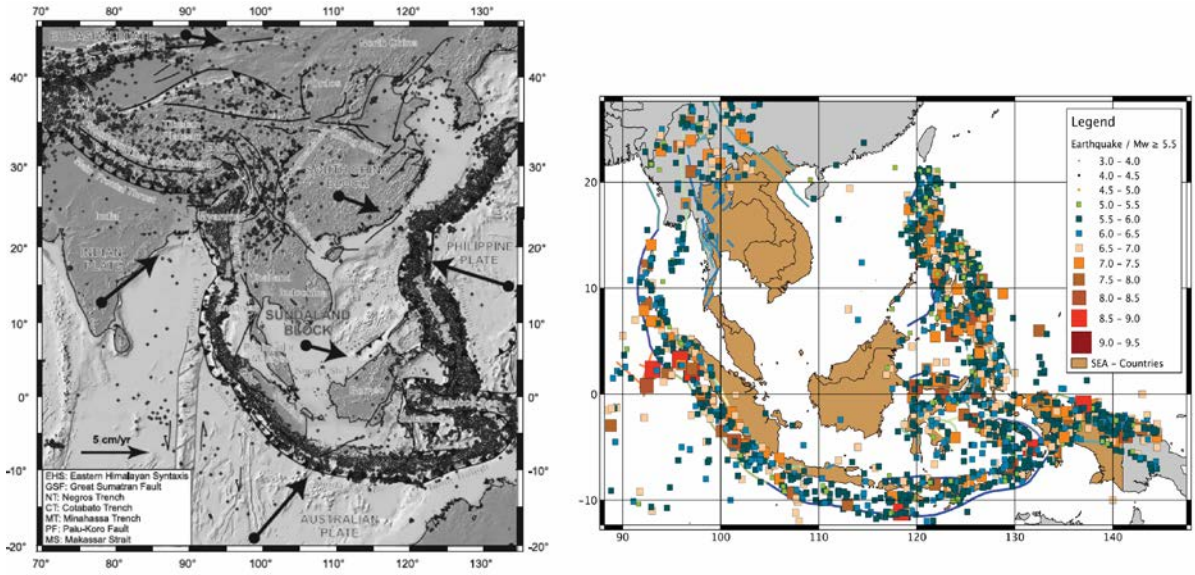

Fig. 2 - (Left) Tectonic overview for SE-Asia as depicted by Simons et al. (2007). (Right) Map of crustal earthquakes with depth d ≤50km and $M_W \geq 5.5$ since 1900.

The Indian-Australian / Australian plate subducts at varying rates and angles between 45-55mm/year beneath the Sunda block, with an oblique direction along the Andaman-Sumatra trench section to a perpendicular direction at the Sunda and Java trench. The change in relative motion links directly to the transform faulting on the island of Sumatra prone to generate large crustal earthquakes. Complexity increases to the southeast of Indonesia, where multiple smaller plates exist due to the collision with the Australian and the Philippine plates, creating multiple smaller plates (Bird, 2003). The tectonic system on in the Molucca and Banda sea extending to Papua New Guinea and northwards to the Philippines remains one of the least understood tectonic systems while converging with slip rates between 30-100mm/y and uncertain plate coupling ratios. The geometry of the bending subduction zone interface around the Banda sea, the double subduction zone of the Sangihe and Halmahera and their interplay are yet to be explained. The Philippine Islands are squeezed in between the Philippine subduction zone moving at up to 100mm/y in the east and the more irregular structures to the west, from Cotabato to the Manila subduction interfaces.

Continental collision occurs in the extend of the Andaman-Subduction to Northern Myanmar generating strong earthquakes at depths down to 100km that contribute to the hazard in Thailand, similar to possible strong strike-slip events along the Sagaing fault in Myanmar. Thailand experiences hazard mainly from basin-opening tectonism on slower slipping strike-slip and normal-faults.

Major intracontinental crustal strike-slip fault systems such as the Sumatra fault zone [30], the Philippine fault zone [18] or the less broadly known Sulu-Sorong and the Palu-Koro fault systems [26–31] act and form the regional tectonics and complicate the partitioning of the ongoing deformation.

Seismicity occurs throughout the known seismically active depth range and concentrates along the subduction zones and the tectonically related crustal faults: from events rupturing along crustal strike-slip faults (~0-40km depth) along the Sumatran fault, to the mega-thrust earthquakes on the subduction interface (~20-60km depth), and to deep focus inslab earthquakes (up to 700km depth) below the Molucca and Banda Sea. These very deep events are not found historically in either the Sunda-Java section or the Andaman-Sumatra section that have recently shown the highest activity and the largest events in the region, such as the December 26, 2004, M_W 9.0 event. Last but not least, the region features some of the most unexpected events. Two examples are the 2012 Wharton basin M8+ event off-Sumatra, the largest strike-slip earthquake ever measured [42], and the 1977

Sumba M8+ normal faulting event in the outer rise of the Java subduction zone segment, that caused severe damage on the Indonesian islands.

2. Data Compilation

2.1 Earthquake catalog

We compiled an earthquake catalog from local and global sources following simple and reproducible rules. The catalog includes earthquakes listed in the IASPEI Cententenniel Earthquake Catalog (1900 - 2002) [16], USGS/NEIC PDE catalog (1973 – 2014.5) at (*http://neic.usgs.gov*), the ISC catalog (1901 - 2012) (*http://www.isc.ac.uk*), 4) and the GCMT (1976 - 2011) [14,15] (Figure 2, right panel).

All catalogs provide in general differencing hypocentral locations and various magnitudes types. Magnitudes of the same type are often not determined with the same algorithms and/or the same base parameters, thus all of them represent also a model of the "observed" seismicity. In a first step we derive a moment magnitude for each event using global scaling relations such as [33,24] and if possible propagate the uncertainties in magnitude and location. We then compile a catalog using simple and hierarchical rules in line with the suggestions by the ISC [13]. We define a preference scheme based on the choice of the catalog, the magnitude within the catalog, and the occurrence time of the event based on which duplicate selection is performed. The catalog is then declustered using windowing approaches to understand sensitivities and clustering foreshock and aftershocks [43]. As an example, less than 40,000 events remain when using the original Gardener and Knopoff (1974) windows (Figure 3).

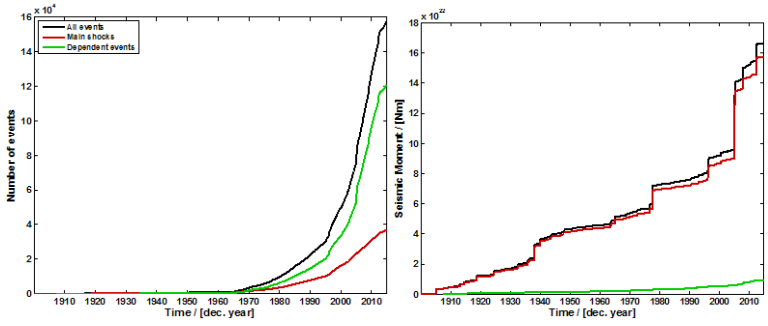

Fig. 3 - Number of events (left) and seismic moment release (right) for the entire compiled catalog as well as main shocks and dependent events. Dependent events include foreshocks and aftershocks.

2.2 Crustal Fault Model (CFM)

Earthquakes occur on faults and the majority of damaging events occur on major fault systems that are known to a certain limit. Several major intra-continental strike-slip fault systems are mapped or are currently being mapped by geological, seismic, or geodetic techniques such as the Sagaing fault in Myanmar [41], the Sumatra fault zone in Indonesia [30] or the Philippine fault zone mapped by scientists of PHIVOLCS and others [40]. However, many more fault systems exist across the area that is less well known yet also capable of causing disastrous events.

We compiled a crustal fault model that includes geometric and kinematic parameters to estimate earthquake activity rates based on multiple approaches. The model includes more about 22000km of surface traces and more than 100 fault sections (Figure 4)**.** Similar to the earthquake catalog, the CFM is a compilation of data from multiple published resources. Faults are included whenever multiple independent sources reported slip rates.

The parameterization allows to generate several different activity rate models: characteristic-type models, moment constrained Gutenberg-Richter type models, and also seismicity based models with earthquakes associated with the fault systems. For each fault zone, a combination will be defined via a logic-tree.

2.3 Subduction Interface Model (SM)

Data quality about the subduction zone geometry varies considerably across the region. Wherever possible, we use the USGS Slab1.0 model [20], otherwise we delineate the interface geometry with simpler approximation using the trench onsets [8] and a predefined constant dip such as provided in [21,6], or use special studies such as for the Manila trench [44]. We evaluate the interface geometry with comparisons to seismicity in cross-sections and results of tomography studies (Fig. 4).

Subduction zone interfaces are characterized as the crustal faults and geometrically complex structures are possible. We use information on plate coupling to infer effective slip rates (Fig.3, colored lines) and thereof recurrence times. In-slab seismicity is treated within the background seismicity model.

The subduction zone interface is modeled within large segments applying a doubly-truncated Gutenberg-Richter model and a characteristic rate model. We use appropriate magnitude area scaling relations to estimate the maximum magnitudes on the defined segments for the characteristic model. Segmentation is based on convergence rate variability, changes in convergence geometry, age of sea-floor and seismic productivity (Fig. .4, dashed grey boxes)

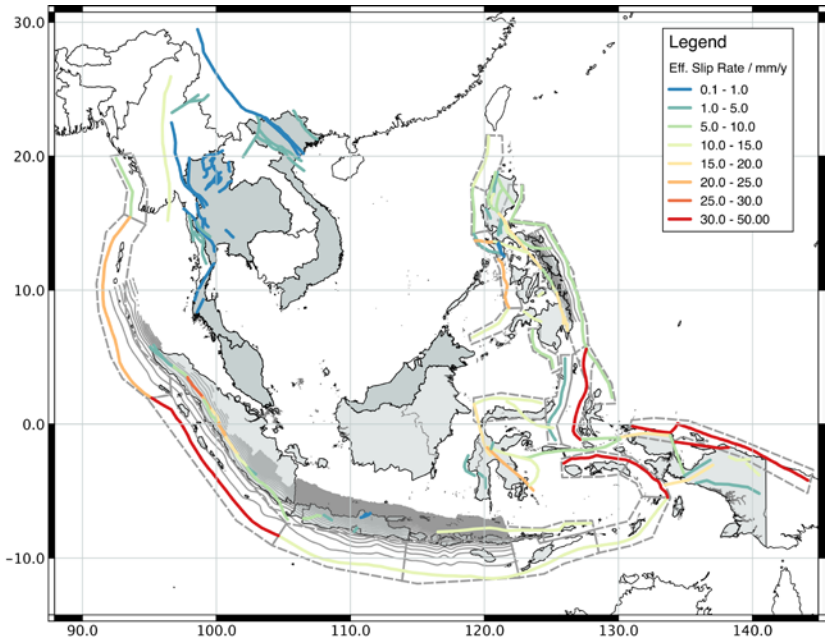

Fig. **4** – Subduction zone interface geometry. Trench locations are colored by effective slip rate.

3. Hazard Modeling

We build a logic-tree based hazard model that combines modeling earthquake rates on unmapped faults, generally called a background model (BGM), activity rates determined from the crustal fault model (CFM) and those from the subduction zone model (SM).

The background seismicity is modeled with smoothed seismicity approach using an adaptive kernel approach as in [43,22] applying an optimized kernel width. We use events that are not associated to any fault or subduction zone within a swatch around the modeled structure of up to 35km. We apply the approach at three depth levels, a crustal layer ($D \leq 50$km), an intermediate layer ($50\text{km} < D \leq 200\text{km}$) and a deep layer ($D > 200$km) while the deep layer is not considered for risk calculations. For each depth layer, the overall activity and b-value with a Gutenberg Richter model. We model regionally different maximum magnitudes of up to $M_W8.9$ to occur in the crustal background of the Indian / Australian plate based on the 2012 Wharton Basin [42] and assume values up to $M_W7.5$ in the Sunda-block region in the crust. The intermediate and deep layers cover mainly inslab earthquakes.

Crustal fault seismicity and subduction interface seismicity are both modelled with doubly-truncated Gutenberg Richter and characteristic type models as evidence for both behaviors exist [7–39] mainly weighted equally. The contributions of the models to the final logic-tree vary per region due to our perspective on the quality of the data and appropriateness of the approach.

4. Ground Motion Model

One of the important components for seismic hazard assessment is a well-selected suite of ground motion prediction equations (GMPEs) that are appropriate for the region of interest and the prevailing tectonic regimes. This is required to 1) accurately capture the median ground motion and its uncertainty and 2) implement source parameters (e.g. earthquake magnitude) and path parameters such as site-to-source distance to define the seismic hazard at a site – that can be represented by peak ground acceleration (PGA) and pseudo-spectral acceleration (PSA) and 3) predict probability of exceedance of strong ground motion parameters.

Despite the many successful efforts to build strong motion networks, e.g. in Indonesia by the Bureau for Meteorology and Geophysics (BMKG) or in the Philippines [24], data availability is scarce especially for building local ground motion prediction models. Thus we utilize the latest models derived from global datasets and similar tectonic regimes whenever possible. The regionalization of tectonic regimes is informed by the basis of the USGS Shakemap approach [19].

Southeast Asia has variable seismic hazard ranging from high seismic hazard associated with subduction zones beneath the Indonesian and Philippine archipelagos to moderately low seismic hazard across large stable region containing the Malaysian peninsula. There is a mix of reverse, thrust, strike-slip and normal-faulting within the region. Therefore, we divided Southeast Asia into three different tectonic settings. Accordingly, we preliminary selected a set of GMPEs that are applicable to each region that covers countries of Indonesia, Malaysia, the Philippines, Singapore, Thailand, and Vietnam. We normalized all GMPEs to reference rock conditions (NEHRP B/C) with time averaged shear-wave velocity within top 30m of soil (V_{S30}) of 760m/s that is compatible with Southeast Asia seismic hazard maps (Building Seismic Safety Council, 2003). The models are validated against 2014 USGS Seismic Hazard Report [29].

4.1. Selection of GMPEs

The scarcity of strong ground motion data in Southeast Asia affects the reliability of GMPEs derived for this region, especially at near-field. This requires a careful selection of local and global GMPEs with comparable regions. We implement GMPEs to three tectonic regimes within Southeast Asia that are crustal interplate earthquakes from stable continental regions, crustal interplate earthquakes near plate boundaries, and interface earthquakes for subduction zones including intermediate and deep earthquakes within the slab. We define the selected GMPEs for each region in the following sub-sections.

4.2. Crustal interplate GMPEs

The GMPEs in this category apply to crustal faulting and differentiate the type of faulting (i.e. strike-slip, normal, reverse/oblique faults). We use NGA-W2 (Next Generation Attenuation for Western United States 2) GMPEs that are applicable to active crustal regions worldwide that include Abrahamson et al. (2014) [1], Boore et al. (2014) [9], Campbell and Bozorgnia (2014) [11], Chiou and Youngs (2014) [12], and Idriss (2014) [46]. We assign equal weights to each GMPE except for Idriss (2014) [46]. The Idriss (2014) model is assigned half the weight as the model does not include nonlinear soil amplification and is applicable only for rock conditions. The applicability ranges of each GMPE are taken into consideration during the model implementation. All five GMPEs are included to capture the epistemic uncertainty.

4.3. Crustal intraplate GMPEs

GMPEs in this category apply to stable Sunda plate and sources in stable continental Australia. We selected following GMPEs that are appropriate for stable continental regions: Toro and others (1997), Toro (2002) [37,38], Frankel and others (1997) [17], Atkinson and Boore (2006') [5], Somerville and others (2001) [35], Campbell (2003) [10], Tavakoli and Pezeshk (2005) [36], Silva and others (2002) [32], and Pezeshk and others (2011) [28]. Weights for each GMPE for different source types such as RLME (Repeated large magnitude

earthquake) and GridSrc (Background gridded sources) are taken from 2014 USGS Seismic Hazard Map document for stable continental regions as shown Table 1. We converted GMPEs that are developed for hard-rock conditions of NEHRP A to NEHRP B/C by applying frequency-dependent factors derived from Frankel et al. (1997) and Atkinson and Boore (2011). The applicability ranges of each GMPE are also taken into consideration during the model implementation.

Table **1** - Weights for Central and Eastern United States GMPEs

GMPE for CEUS	Weight	
	RLME	GridSrc
Atkinson (2008')	0.08	0.08
Atkinson and Boore (2006')	0.22	0.25
Campbell (2003)	0.11	0.13
Frankel and others (1996)	0.06	0.06
Pezeshk and others (2011)	0.15	0.16
Silve and others (2002)	0.06	0.06
Somerville and others (2001)	0.10	0.00
Tavakoli and Pezeshk (2005)	0.11	0.13
Toro and others (1997), Toro (2002)	0.11	0.13

4.4. Subduction Zone GMPEs

Among the available GMPEs for subduction seismic sources, we use globally developed subduction zone GMPEs that contain Zhao and others (2006) [45], Atkinson and Boore (2003) [3], and Abrahamson et al. (2015) [2]. The weights are assigned based on Trellis plots that allow us to examine 1) magnitude scaling for different distance, hypocentral depth and spectral period bins, 2) distance scaling for different magnitude and period bins, 3) spectral shape for various magnitude and distance combinations, and 4) between- and within-event aleatory uncertainty terms. The applicability ranges of each GMPE are also taken into consideration during the model implementation. We also investigated the usage of Adnan and others (2014) that is specific for Peninsular Malaysia.

5. Hazard Results

Preliminary seismic hazard for 10% exceedance probabilities in 50 years (average return period of 475y) for rock conditions (V_{S30}=760m/s) reach up to 1.2g in several regions across South-East Asia, particularly along the subduction interfaces and the fast slipping crustal faults. Within the stable Sunda block and in continental South-East Asia the hazard is comparatively low, however, not negligible in terms of risk as cities like Hanoi (Vietnam) locate along well known structures. The recurrence of large earthquakes and the modeling of the ground motions in these regions is hampered by the large uncertainties on fault movement measurements and limited detailed information resulting in considerable uncertainty compared to detailed studied fault systems such as the Sumatra fault zone [30].

Focusing on the largest cities in high hazard regions, we display uniform hazard spectra for locations in Manila (Philippines) and Jakarta Utara (Indonesia) (Fig. 5). Hazard values a higher in Manila compared to Jakarta; while Manila hazard is dominated by subduction interface events on the Manila Trench and events on the Marikina Valley fault, hazard in Jakarta is dominated by intermediate depth (50-250km) and subduction interface events. While for both the hazard values are considered moderate on base rock, amplification effects are expected to be strong, as both metropolitan areas are located in sediment basins.

Fault systems and subduction zone environments prominently contribute to the seismic hazard in Indonesia and the Philippines (Fig. 5). Hazard levels for continental SE Asia and on the Sunda block islands are much lower compared to the Indonesia and the Philippines, yet with differences. While many possible fault sources have been assessed for continental SE Asia (Fig. 6), the hazard is dominated by background seismicity in continental for PGA as most of the faults are assigned low slip rates and seismic activity is sparse towards the coast of

Thailand and Vietnam. For the latter, prominent fault structures like the Red River fault system contribute to more prominently to longer return period hazard.

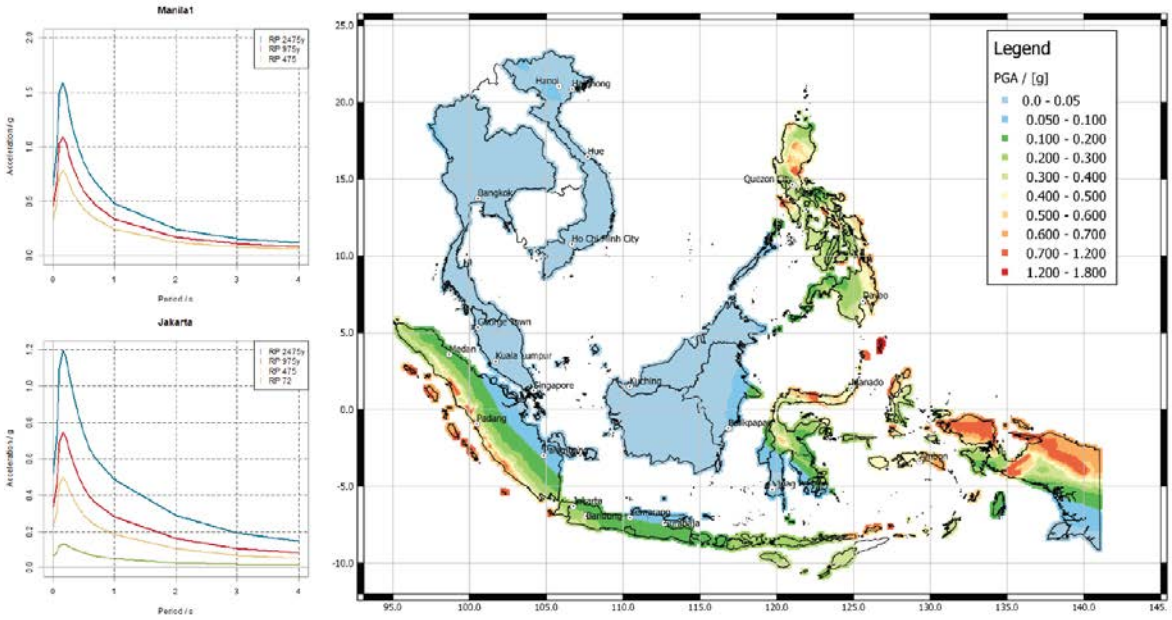

Fig. **5** – Hazard results: (left) Uniform hazard spectra for a location in Manila (Philippines) and Jakarta-Utara (Indonesia) for PGA at three return periods. (right) Seismic hazard map for South-East Asia (PGA, 475y return period). Both for reference rock velocity of V_{S30}=760m/s.

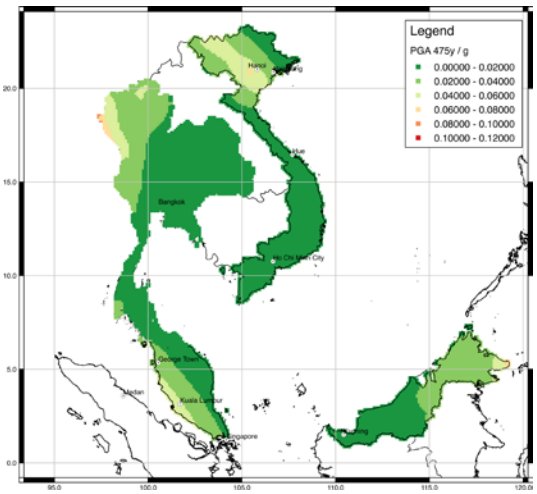

Fig. 6. - Seismic hazard map for continental South-East Asia (PGA, 475y return period) for reference rock velocity of V_{S30}=760m/s.

6. A Glance on the Economic Impact

Seismic hazard estimates are an important intermediate step when estimating seismic risk for comparison and evaluation of the model before calculating losses. Folding in an exposure database, a vulnerability model as well as an appropriate financial model (Fig. 1) leads to risk estimates valuable for the financial industry often expressed as expected average annual loss (AAL).

Fig. 7 shows percentage contributions of earthquake source model parts to the AAL for Indonesia and the Philippines. The comparison reveals a higher percentage of contributions from subduction interface and inslab / deep events for Indonesia than for the Philippines, while contributions from crustal faults are larger in the Philippines. This relates to the source model (Fig. 2) as crustal fault coverage in the Philippines is relatively larger than in Indonesia, especially near the exposure concentrations of Manila when compared to Jakarta. The distribution in Fig. 7 is a countrywide overview, however, spatially the relative contributions can vary substantially across the countries.

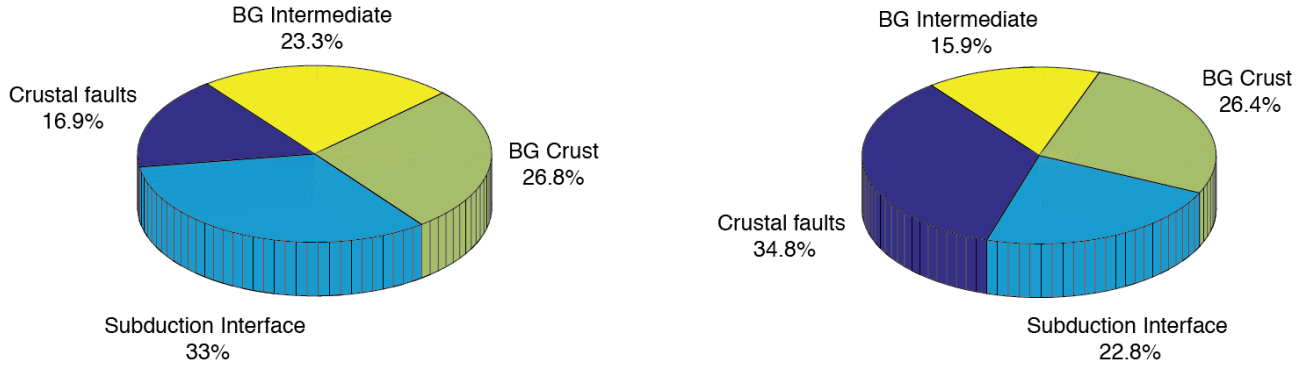

a) Indonesia b) Philippines

Fig. **6** – Percentage contributions of source model parts to Average Annual Loss (AAL) for Indonesia and Philippines.

7 References

[1] Abrahamson NA, Silva WJ, Kamai, R (2014). NGA-West 2 equations for predicting PGA, PGV, and 5%-damped PSA for shallow crustal earthquakes. Earthq Spectra, 30, 3, 1025-1055.

[2] Abrahamson, N, Gregor, N, Addo K (2015). BC Hydro ground motion prediction equations for subduction earthquakes. Earthq Spectra, Preprint, (-Not available-) pp.

[3] Atkinson, GM, Boore, DM (2003). Empirical ground-motion relations for subduction-zone earthquakes and their application to Cascadia and other regions, Bull Seismol Soc Am, Vol. 93, 1703-1729.

[4] Atkinson, GM, Boore, DM (2006). Earthquake ground-motion prediction equations for eastern North America: Bull Seismol Soc Am, v. 96, p. 2,181–2,205, doi:10.1785/0120050245.

[5] Atkinson, GM and Boore, DM (2011). Modifications to existing ground-motion prediction equations in light of new data: Bull Seismol Soc Am, v. 101, p. 1,121–1,135, doi:10.1785/0120100270.

[6] Berryman K, Wallace L, Hayes G, Bird P, Wang K, Basili R, et al (2013). The GEM Faulted Earth Subduction Characterisation Project (Version 1.0).

[7] Bilek SL, Satake K, Sieh K (2007) Introduction to the Special Issue on the 2004 Sumatra-Andaman Earthquake and the Indian Ocean Tsunami. Bull Seismol Soc Am 97:S1–S5. doi: 10.1785/0120050633.

[8] Bird P (2003). An updated digital model of plate boundaries. Geochemistry, Geophys Geosystems;4:n/a – n/a. doi:10.1029/2001GC000252.

[9] Boore, DM, Stewart, JP, Seyhan, E, and Atkinson, GM (2014). NGA-West 2 equations for predicting PGA, PGV, and 5%-damped PSA for shallow crustal earthquakes, Earthq Spectra, 30, 3, 1057-1085.

[10] Campbell, KW (2003). Prediction of strong ground motion using the hybrid empirical method and its use in the development of ground motion (attenuation) relations in eastern North America: Bull Seismol Soc Am, v. 93, p. 1,012–1,033.

[11] Campbell, KW, Bozorgnia, Y (2014). NGA-West2 Ground Motion Model for the Average Horizontal Components of PGA, PGV, and 5%-Damped Linear Acceleration Response Spectra, Earthq Spectra,30, 3, 1087-1115.

[12] Chiou, SJ and Youngs, RR (2014). Update of the Chiou and Youngs NGA model for the average horizontal component of peak ground motion and response spectra, Earthq Spectra,30, 3, 1117-1153.

[13] Di Giacomo D, Storchak DA (2016). A scheme to set preferred magnitudes in the ISC Bulletin. J Seismol;20:555–67. doi:10.1007/s10950-015-9543-7.

[14] Dziewonski AM, Chou T-A, Woodhouse JH (1981). Determination of earthquake source parameters from waveform data for studies of global and regional seismicity. J Geophys Res;86:2825. doi:10.1029/JB086iB04p02825.

[15] Ekström G, Nettles M, Dziewoński AM (2012). The global CMT project 2004–2010: Centroid-moment tensors for 13,017 earthquakes. Phys Earth Planet Inter;200-201:1–9. doi:10.1016/j.pepi.2012.04.002.

[16] Engdahl ER, Villaseñor A (2002). Global seismicity - 1900-1999. Int. Handb. Earthq. Eng. Seismol., Amsterdam: Academic Press; pp. 665–90.

[17] Frankel, A, Mueller, C, Barnhard, T, Perkins, D, Leyendecker, EV, Dickman, N, Hanson, S, and Hopper, M (1996). National seismic hazard maps—Documentation June 1996: U.S. Geological Survey Open-File Report 96-532, 110 p.

[18] Galgana G, Hamburger M, McCaffrey R, Corpuz E, Chen Q (2007). Analysis of crustal deformation in Luzon, Philippines using geodetic observations and earthquake focal mechanisms. Tectonophysics;432:63–87. doi:10.1016/j.tecto.2006.12.001.

[19] Garcia D, Wald DJ, Hearne MG (2012). A Global Earthquake Discrimination Scheme to Optimize Ground-Motion Prediction Equation Selection. Bull Seismol Soc Am;102:185–203. doi:10.1785/0120110124.

[20] Hayes GP, Wald DJ, Johnson RL (2012). Slab1.0: A three-dimensional model of global subduction zone

geometries. J Geophys Res;117:B01302. doi:10.1029/2011JB008524.

[21] Heuret A. Physical characteristics of subduction interface type seismogenic zones revisited n.d. doi:10.1029/2010GC003230.

[22] Hiemer S, Woessner J, Basili R, Danciu L, Giardini D, Wiemer S (2014). A kernel-smoothed stochastic earthquake rate model considering seismicity and fault moment release for Europe. Geophys J Int;198. doi:10.1093/gji/ggu186.

[23] Lolli B, Gasperini P, Vannucci G (2014). Empirical conversion between teleseismic magnitudes (mb and Ms) and moment magnitude (Mw) at the Global, Euro-Mediterranean and Italian scale. Geophys J Int;199:805–28. doi:10.1093/gji/ggu264.

[24] Melosantos AA, Soriano KVC, Alcones PCM, Pantig JU, Bonita JD, Narag IC, et al (2015). Performance of Broadband Seismic Network of the Philippines. J DisasterResearch;10:8–17.

[25] Meltzner AJ, Sieh K, Chiang H-W, Wu C-C, Tsang LLH, Shen C-C, et al (2015). Time-varying interseismic strain rates and similar seismic ruptures on the Nias–Simeulue patch of the Sunda megathrust. Quat Sci Rev;122:258–81. doi:10.1016/j.quascirev.2015.06.003.

[26] Molnar P, Dayem KE (2010). Major intracontinental strike-slip faults and contrasts in lithospheric strength. Geosphere;6:444–67. doi:10.1130/GES00519.1.

[27] Ornthammarath T, Warnitchai P. (2016). The 5 May 2014 MW 6.1 Mae Lao (Northern Thailand) earthquake: Interpretations of recorded ground motion and structural damage. Earthq Spectra.

[28] Pezeshk, S, Zandieh, A, and Tavakoli, B (2011). Hybrid empirical ground-motion prediction equations for eastern North America using NGA models and updated seismological parameters: Bull Seismol Soc Am, v. 101, p. 1,859–1,870, doi:10.1785/0120100144.

[29] Petersen, M, Moschetti, MP, Powers, PM, Mueller, CS, Haller, KM, Frankel, AD, Zeng, Y, Rezaeian, S, Harmsen, SC, Boyd, OS, Field, N, Chen, R, Rukstales, KS, Luco, N, Wheeler, RL, Williams, RA, Olsen, AH. (2014). Documentation for the 2014 Update of the United States National Seismic Hazard Maps, Open-File Report 2014–1091.

[30] Sieh K, Natawidjaja D. (2000). Neotectonics of the Sumatran fault, Indonesia. J Geophys Res;105:28295. doi:10.1029/2000JB900120.

[31] Simons WJF, Socquet A, Vigny C, Ambrosius BAC, Haji Abu S, Promthong C, et al (2007). A decade of GPS in Southeast Asia: Resolving Sundaland motion and boundaries. J Geophys Res;112:B06420. doi:10.1029/2005JB003868.

[32] Silva, W, Gregor, N, Darragh, R (2002). Development of regional hard rock attenuation relations for central and eastern North America: Pacific Engineering and Analysis Technical Report, 57 p.

[33] Sipkin SA (2003). A Correction to Body-wave Magnitude mb Based on Moment Magnitude Mw. Seismol Res Lett;74:739–42. doi:10.1785/gssrl.74.6.739.

[34] Socquet A, Simons W, Vigny C, McCaffrey R, Subarya C, Sarsito D, et al (2006). Microblock rotations and fault coupling in SE Asia triple junction (Sulawesi, Indonesia) from GPS and earthquake slip vector data. J Geophys Res;111:B08409. doi:10.1029/2005JB003963.

[35] Somerville, P, Collins, N, Abrahamson, N, Graves, R, Saikia, C (2001). Ground motion attenuation relations for the Central and Eastern United States—Final report, June 30, 2001: Technical report to U.S. Geological Survey, Reston, Virginia, under Contract 99HQGR0098, 38 p.

[36] Tavakoli, B, Pezeshk, S (2005). Empirical-stochastic ground-motion prediction for eastern North America: Bull Seismol Soc Am, v. 95, p. 2,283–2,296.

[37] Toro, GR, Abrahamson, NA, Schneider, JF (1997). Model of strong ground motions from earthquake in central and eastern North America—Best estimates and uncertainties: Seism Res Letters, v. 68, p. 41–57.

[38] Toro, GR (2002) Modification of the Toro et al. Attenuation equations for large magnitudes and short distances: Risk Engineering Technical Report, 1997, 10 p.

[39] Tormann T, Enescu B, Woessner J, Wiemer S (2015). Randomness of megathrust earthquakes implied by rapid stress recovery after the Japan earthquake. Nat Geosci;8:152–8. doi:10.1038/ngeo2343.

[40] Tsutsumi H, Daligdig JA, Goto H, Tungol NM, Kondo H, Nakata T, et al (2006). Timing of surface-ruptureing earthquakes on the Philippine fault zone in central Luzon Island. Eos Trans. Am. Geophys. Union.

[41] Wang Y, Sieh K, Tun ST, Lai K-Y, Myint T (2014). Active tectonics and earthquake potential of the Myanmar region. J Geophys Res Solid Earth;119:3767–822. doi:10.1002/2013JB010762.

[42] Wei S, Helmberger D, Avouac J-P (2013). Modeling the 2012 Wharton basin earthquakes off-Sumatra: Complete lithospheric failure. J Geophys Res Solid Earth;118:3592–609. doi:10.1002/jgrb.50267.

[43] Woessner J, Laurentiu D, Giardini D, Crowley H, Cotton F, Grünthal G, et al (2015). The 2013 European Seismic Hazard Model: key components and results. Bull Earthq Eng. doi:10.1007/s10518-015-9795-1.

[44] Yu S-B, Hsu Y-J, Bacolcol T, Yang C-C, Tsai Y-C, Solidum R (2013). Present-day crustal deformation along the Philippine Fault in Luzon, Philippines. J Asian Earth Sci;65:64–74. doi:10.1016/j.jseaes.2010.12.007.

[45] Zhao, JX, Zhang, J, Asano, A, Ohno, Y, Oouchi, T, Takahashi, T, Ogawa, H, Irikura, K, Thio, HK, Somerville, PG, Fukushima, Y, Fukushima Y. Attenuation relations of strong ground motion in Japan using site classification based on predominant period, Bull Seismol Soc Am, Vol. 2006, 96, 898-913.

[46] I. M. Idriss (2014). An NGA-West2 empirical model for estimating the horizontal spectral values generated by shallow crustal earthquakes, Earthquake Spectra, 30(3):1155–1177, 2014. doi: 10.1193/070613EQS195M.

[47] A. Adnan, AV Shoustari, NSH Harith (2014) On the Selection of Ground-Motion Prediction Equations Compatible with Peninsular Malaysia Region for Sumatran Subduction In-Slab Earthquakes. Jour. of Civil Eng. Res. 4(3A): 124-129.